COBEM 2021 26th International Congress of Mechanical Engineering
November 22-26, 2021, Virtual Congress, Brazil

COB-2021-2083
EVALUATION OF THE SIGMA PHASE CONTENT IN MULTI-PASS WELDING OF STAINLESS STEEL DUPLEX UNS S31803 VIA LINEAR SWEEP VOLTAMMETRY TECHNIQUE

Elan Gabriel Forteski
Luiz Otávio Rigobello Muraro
Carolina Mocelin Gomes Pires
Maria José Jerônimo de Santana Ponte
Haroldo Araújo Ponte
Federal University of Parana, Laboratory of Electrochemistry of Surfaces and Corrosion (LESC), 81530-000 Curitiba, Brazil
elangabriel@ufpr.br
luizotaviorigobello@gmail.com
carolinamocelin@ufpr.br
mponte@ufpr.br
hponte@ufpr.br

Abstract. *Duplex stainless steels are materials that have good mechanical properties and corrosion resistance due to microstructural synergy in similar volumetric fractions of ferrite and austenite. However, when these materials are subjected to thermal aging or welding processes, local changes in their composition can occur and generate undesirable intermetallic phases, such as the sigma phase. This condition can lead to embrittlement of the material and, consequently, loss of tenacity and reduction of resistance to pitting corrosion. In light of this view, the aim of the present work was to quantify the sigma phase due to welding process of duplex stainless steels UNS S3180 and to evaluate these contents via the linear sweep voltammetry technique. To that end, samples were submitted to MIG/MAG multipass welding processes. The results obtained by optical microscopy showed that the formation of the deleterious intermetallic phase occurred with the increase in the number of weld pass. Therefore, it was observed that the highest concentration of sigma phase was that of last welding weld pass, at the material surface. This condition allows us to use the linear sweep voltammetry technique, a surface technique, to quantify the intermetallic phase, as a non-destructive method. The results of this quantification technique detected contents of about 0.45% of sigma phase per unit of area, much lower than the 1.00% considered as critical level.*

Keywords*: non-destructive testing, linear sweep voltammetry technique, intermetallic phases, corrosion.*

1. INTRODUCTION

Stainless steels are corrosion-resistant ferrous alloys. Such steels have been developed in Germany and the United Kingdom in the first decades of the XXth century and overtime they have undergone several microstructural changes until reaching the standards of present-day alloys. An example of those is the duplex stainless steels (DSS), which are widely known for their excellent mechanical properties and for their resistance to corrosion (GUNN, 1997). DSS, as well as other stainless steels, have the ability to generate a surface layer, known as passivating film, consisting of chromium oxides. That film is self-generating and, consequently, reduces the oxidation reaction rate between the metal and the medium (OLSSON; LANDOLT, 2003). This behavior allows its use in aggressive environments, such as subsea pipelines, chemical mixing tanks, and other components of the industry. (JEBARAJ et al., 2017).

The DSS microstructure consists of two phases: ferrite (α) and austenite (γ). Unnikrishnan and Mallik (1987) state that in order to establish the best mechanical properties and resistance to corrosion, the alloy must present the α and γ phases in equivalent volumetric ratios. As a result, the high corrosion resistance of the DSS is related to the alloying elements (Ni, Mn, N, Cr, Mo, and Si), which directly influenced the steel microstructure.

Although the alloy elements provide several positive characteristics to the steels, when the DSSs are submitted to thermal processes they become susceptible to the precipitation of harmful intermetallic phases, such as the sigma phase (σ). This phase can decrease the mechanical properties and corrosion resistance of steels (GARCÍA-RENTERÍA et al., 2014). The precipitation of this intermetallic phase occurs in temperatures between 600ºC and 1000ºC (KARLSSON, 2012), and the degradation in the material microstructure occurs with contents starting at 1% of the σ-phase.

In the industrial context, steel welding processes provide a large thermal input to the material and, during this stage, the σ-phase precipitation may occur. The MIG/MAG-type welding method is widespread in the industrial area. This is due to the easy use of the materials for welding, the possibility of mechanization of the process and for presenting high yield rates. According to Karlsson (2012), the recommended energy to be applied in DSS UNS S31803 lies between

0.5 kJ mm^{-1} and 2.5 kJ mm^{-1}. Dominices et al. (2020) have observed the formation of the σ-phase for that steel submitted to the MIG/MAG-type weld with a welding energy close to 0.761 kJ mm^{-1}.
In certain industrial applications, it is necessary that the welding occurs in multi weld pass. As a result, the heat-affected zone (HAZ) of the material undergoes different thermal cycles throughout the procedure. In this process, a change in the local microstructure can occur at each welding weld pass performed, allowing the precipitation of different types and concentrations of intermetallic phases (Granjom, 1991). Therefore, monitoring and detecting intermetallic phases in the welded DSSs has been a challenger. For that, Non-Destructive Tests (NDT) are presented as a good alternative to destructive detection tests, since they have the advantage of time to detection and not damaging the material to be analyzed (BIEZMA et al., 2021).

Among the developed NDT, the method via Linear Sweep Voltammetry (LSV), with selective electrolytes, is presented as a high sensitivity technique for detecting quantitatively low contents of σ-phase in stainless steels (Haskel et al. 2019; Forteski 2020). LSV is based on the potential difference generated between the working electrode and the reference electrode, both immersed in an electrolyte solution (BARD and FAULKNER, 2001). Forteski (2020) evaluated the presence of σ-phase in DSS UNS S31803 via LSV. In his work it was observed that the technique was able to detect contents of up to 0.04% of the intermetallic phase per unit area.

Based on a good detection sensitivity of σ-phase using LSV and on the need for detecting the intermetallic phase in steels submitted to high temperatures, the aim of the present work was to evaluate the formation profile of the σ-phase in UNS S31803 steels submitted to different numbers of weld pass. Thus, the present work proposes to employ a non-destructive test (LSV) to quantify the intermetallic phase, which occurs on the surface of the weld region, in order to validate the use of the LSV technique for field application in welded materials in the industry.

2. METODOLOGY

The welded material used – the base metal – was a DSS UNS S31803, obtained from hot rolled sheets, with initial dimensions of 50 mm x 50 mm x 8.5 mm. Aiming at characterizing the base metal and ensure its adequacy to the standard norm (Specification for Stainless Steel Bars and Shapes – ASTM A 276-02 A), an Energy-Dispersive X-ray Spectroscopy – EDX test was performed, and the characterization of the material is presented in Table 1. The filler material used in the welding process was also a DSS UNS S31803.

Table 1– Quantification of DSS UNS S31803 via EDX

Alloy elements					
Carbon (C)	Oxygen (O)	Chromium (Cr)	Iron (Fe)	Nickel (Ni)	Molybdenum (Mo)
1.17%	0.64%	22.17%	66.55%	6.26%	3.21%

Figure 1 schematically presents the assembly of the experimental apparatus used in the process of welding the samples. Welding was conducted in beveled pieces with a 30º angle, according to the methodology proposed by Moteshakker and Danaee (2016).

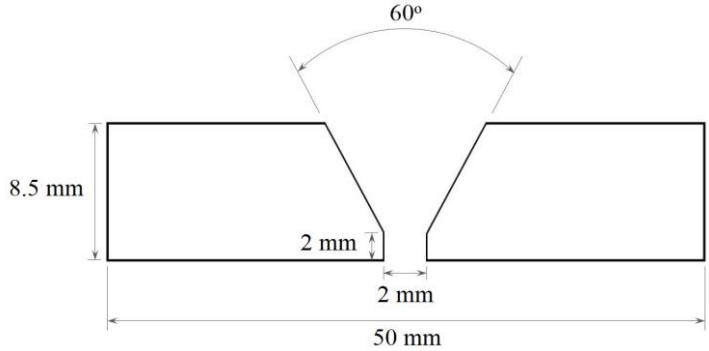

Figure 1 – Welding angle between parts

The samples used in the present work were submitted to different MIG/MAG-type welding pass. Sample M1 contains 1 weld pass, M2 contains 2 weld passes, and M3 contains 3 weld passes. A sample of the base metal – labeled 'Blank' – was also separated, which was not subjected to any welding process. The welding parameters used in the three samples are showed in the Table 2.

'

Table 2 - Welding parameters

Voltage	15-20 V
Current	65-85 A
Welding speed	0.61 mm s^{-1}
Thermal efficiency	0.75
Welding energy	1.57-1.60 kJ mm^{-1}
Shielding gas	Argon [80%]
	CO_2 [20%]
Preheating temperature	100 °C
Interpass temperature	150-200 °C
Filler Metal	ER 2209
Wire diameter	1 mm
Number pass	1, 2 and 3

In order to inhibit the presence of deleterious phases previously to the welding process of the samples, the base metal was solubilized at 1100°C for 10 min. The welded samples were cut in a cross section at the welding line. Subsequently, these samples were sanded in sequential granulometries (120, 220, 400, 600, and 1200 mesh), finishing with alumina with an average granulometry of 0.3 μm. In order to visualize the phases, present in the cutter section, an electrochemical attack was conducted, as shown in Figure 2. In this test, a solution of potassium hydroxide (KOH) (Neon – 85%) was used in a 0.1 mol L^{-1} concentration, and the electric potential applied was 2.5 V for 40 s.

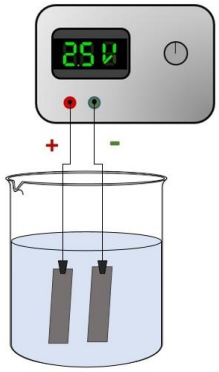

Figure 2 – Experimental apparatus for an electrochemical attack

In order to determine the amount of σ-phase presented in the samples, optical microscopy (Olympus BX51M) were performed. The acquisition of images was carried out via software OIM ANALYSIS 5.0 and, subsequently, the images were submitted to surface area quantification for specific phases via an IMAGE J™ binary counting software.

As an alternative to quantification via optical microscopy (OM) and aiming to use a technique that is not destructive to the material under analysis, the present work proposes the use of the LSV electrochemical test. This test follows the methodology proposed at Forteski (2020) and is schematically shown in Figure 3.

.

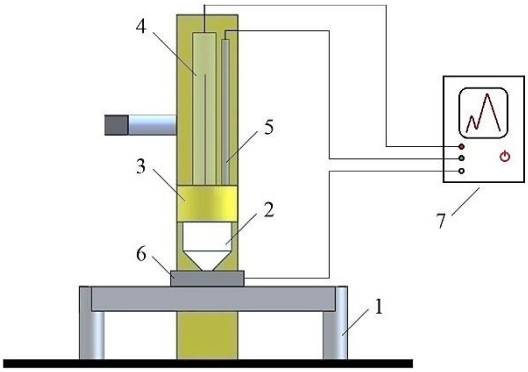

Figure 3 – Experimental apparatus used in LSV containing: 1 – support base; 2 – electrolytic cell; 3 – fixation support; 4 – reference electrode, 5 – auxiliary electrode (platinum), 6 – working electrode (UNS S31803); 7 – electrochemical interface equipment (Palmsens2)

The LSV test was used in the HAZ areas of the last weld pass region for samples M1, M2, M3, and Blank. To carry out voltammetry, an electrolytic solution in a 4 mol L^{-1} concentration was used applying the scanning speed of 0.5 mV s^{-1}. The electrolytic cell, which follows a Luggin capillary concept, has a 0.3318 mm^2 work electrode-solution contact area.

3. RESULTS AND DISCUSSION

After the welding process, the samples were prepared for the metallographic analysis. Specific areas of analysis were defined, which were the weld fusion region and the HAZ, according to Granjom (1991). Figure 4 presents the subdivision of the cut area – in which regions 1, 2, and 3 represent the fusion zone. Region 1 corresponds to the first weld pass, 2 represents the second weld pass, and 3 refers to the third weld pass.

Regions 4, 5, and 6 define the HAZ in the temperature range susceptible to deterioration for each weld pass. The region of base metal away from the weld fusion zone and the HAZ was not considered within the scope of the present work because it was not submitted to significant temperature gradients that could favor the σ-phase precipitation.

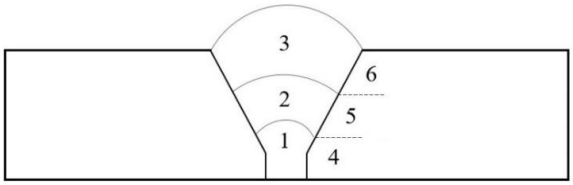

Figure 4 – Welding sequence for 3 weld passes including HAZ

Through the analysis via OM it was observed that sample M1, which has only one weld pass, presented a greater σ-phase nucleation in the HAZ than in the weld fusion zone, as shown in Figure 5.

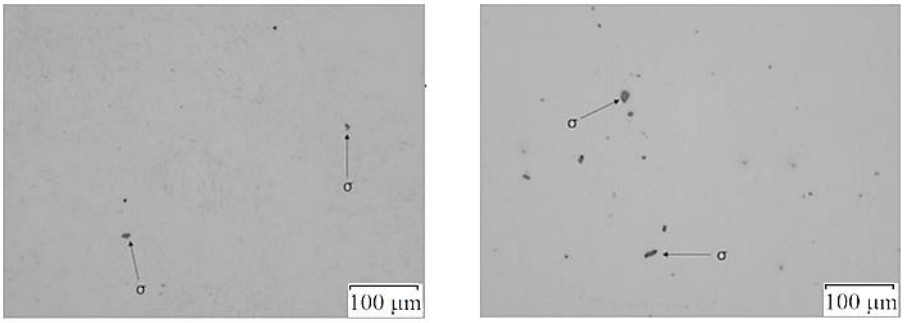

(a) (b)

Figure 5 – Optical microscopy sample M1 in: (a) weld fusion zone; and (b) HAZ

For the sample that has two weld pass (M2), it was observed that HAZ of the second weld pass presented a greater σ-phase than the weld fusion zone of the same weld pass (Figure 6). On the other hand, when comparing the formation of the intermediate phase in each weld pass of sample M2 (Figure 6 and Figure 7), it is observed that the σ-phase concentration, in the HAZ and in the weld fusion zone, was higher in the second weld pass when compared to that of the first weld pass.

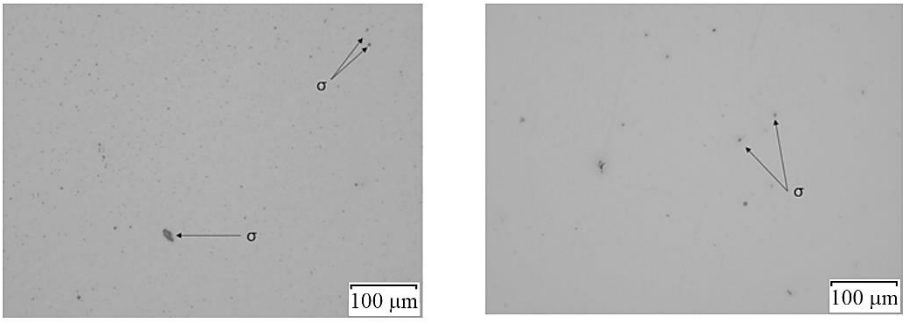

(a) (b)

Figure 6 – Optical microscopy of sample M2 of the first weld pass in: (a) weld fusion zone and (b) HAZ

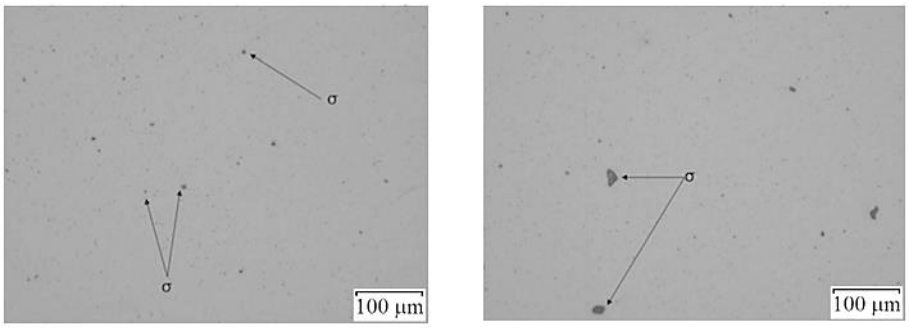

(a) (b)

Figure 7 – Optical microscopy of sample M2 of the second weld pass in: (a) weld fusion zone and (b) HAZ

The results of the analysis of the sample with three weld passes (M3) were similar to those of the previous case (M2). Thus, it follows that, for the last weld pass, sample M3 presented a greater quantity of σ-phase nuclei in the HAZ when compared to the region of the weld fusion zone. When comparing nucleation of the intermetallic phase among the internal weld pass, it was observed that the third weld pass contains a greater σ-phase concentration, as shown in Figure 6 and Figure 7.

Samples M2 and M3 showed a greater σ-phase concentration in the region of the last weld pass, results that may be related to a longer exposure time of the samples to high temperatures, which contributes to the increase of the intermetallic phase in the region of the last weld pass.

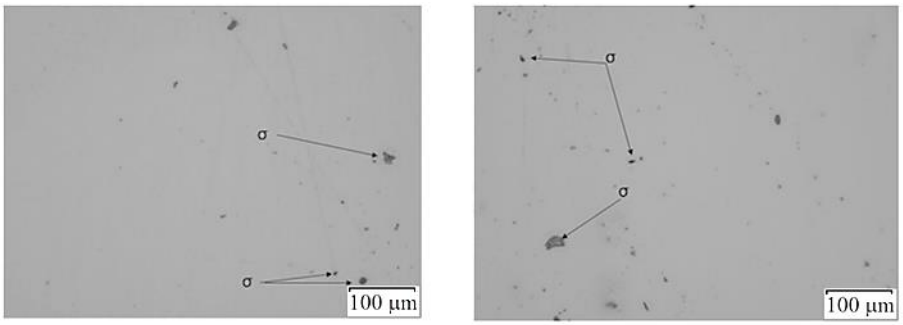

(a) (b)

Figure 8 – Optical microscopy of sample M3 of the first weld pass in: (a) weld fusion zone and (b) HAZ

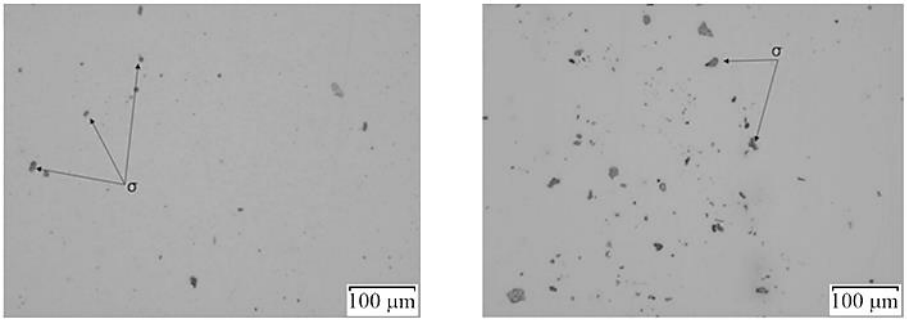

(a) (b)

Figure 9 – Optical microscopy of sample M3 of the third weld pass in: (a) weld fusion zone and (b) HAZ

When analyzing Figure 5 to Figure 9, it can be observed that the nucleation of the σ-phase occurred at the interface between phases α and γ and developed within phase α. The morphological aspect of a coral like structure in HAZ of sample M3 (Figure 9b) was also observed, which has the greater number of weld pass. Such behavior can be related to this region been submitted to lower temperature gradient at the cooling stage, thus favoring the development of intermetallic phase in that region.

In the present work, it was observed that there was a decrease in the σ-phase content in the previous weld pass when the base metal was submitted to a new weld pass. Such behavior may be associated to the increase in temperature – of the weld fusion zone and HAZ – of the DSS due to the energy inputs in thermal cycle. Thus, it is reasonable to admit that there was a solubilization of the intermetallic phase in the previous weld pass because it was subjected to an increase in the local temperature. Considering this very principle, the increase in the σ-phase concentration in the last weld pass may be related to the occurrence of high temperatures due to the very welding process, which favors the formation of the intermediate phase. (Almeida *et al*., 2019). However, in this work we weld pieces of DSS that present small dimensions (50 mm x 50 mm x 8.5 mm), which contributes to the increase of the temperature. On the other hand, it should be considered that welding process in DSS with different dimensions may present different behaviors.

In order to quantify the σ-phase present in the region affected by the welding process, the weld fusion zone and the HAZ, samples M1, M2, and M3 were cut in cross section at the weld line. Thus, to measure the percentage of intermetallic phase in the cut region, the IMAJE J^{TM} software was used. The results are presented in Table 3.

Table 3 – Quantification of σ-phase present in samples M1, M2, and M3

Samples	**Weld fusion zone**	**HAZ (%)**
M1	0.165	0.456
M2 – 1° weld pass	0.398	0.087
M2 – 2° weld pass	0.362	0.539
M3 – 1° weld pass	0.244	0.622
M3 – 3° weld pass	0.472	1.569

According to Table 2, it was observed that the regions of the last weld pass presented a higher σ-phase concentration. The LSV technique is based on the interfacial phenomena between the working electrode surface (metal base) and the electrolytic solution. Such methodology becomes applicable to the quantification of the σ-phase of the samples under study by the present work, since it is a non-destructive technique which allows the quantification of the samples in the surface of the material. Considering that the HAZ of the samples presented higher σ-phase contents, this region was chosen for quantification via LSV.

LSV were performed in duplicate, named run 1 and run 2, and the results presented in Figure 10. The σ-phase-free sample (Blank) showed a peak potential (E_p) of 480 mV and peak current (I_p) of 60 µA. The other voltammograms showed that sample M1, which has 0.45% of σ-phase, presented 66 µA of I_p, representing a 10% increase in relation to the I_p of Blank. On the other hand, the peak potential (E_p) occurred at 473 mV. Sample M2, with 0.54% of σ-phase, obtained I_p = 69 µA, representing a 15% increase in relation to Blank. In this case, there was also a reduction in the E_p value, which occurred at 465 mV. The greater change occurred in M3, which has the largest fraction of precipitates (1.54%), representing I_p = 72 µA. This condition represents a 20% increase in relation to I_p of Blank. However, the E_p value registered for this sample was 456 mV.

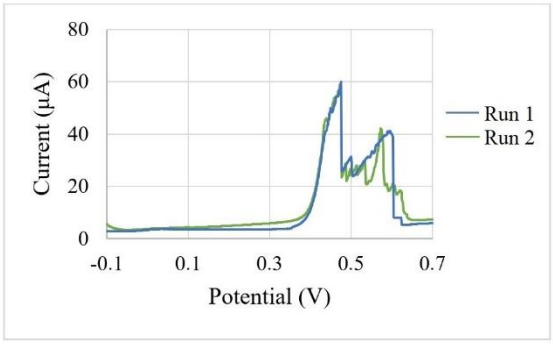

(a)

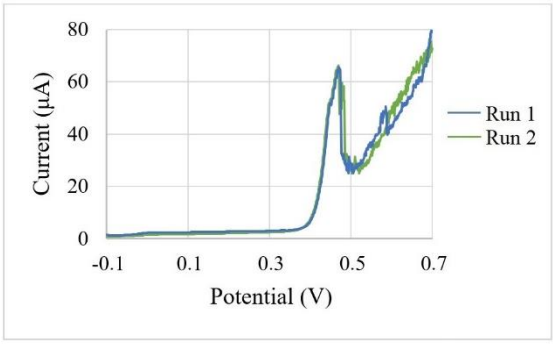

(b)

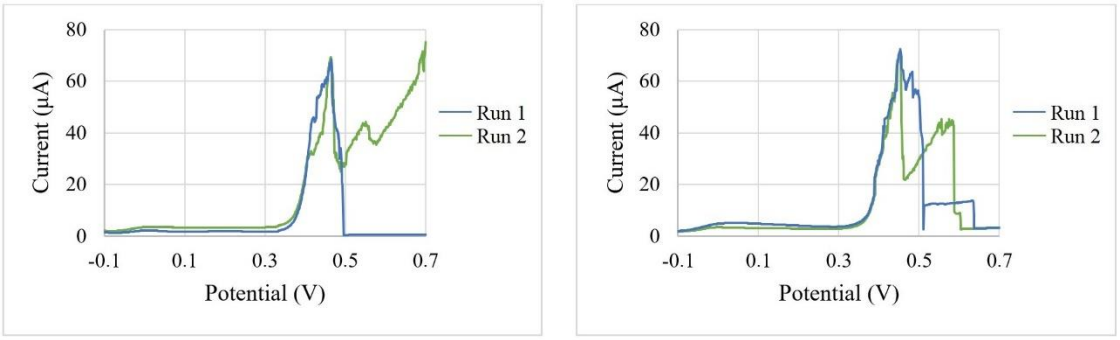

(c) (d)

Figure 10 – Voltammetry of samples in duplicate (Run 1 and Run 2) for: (a) Blank, (b) M1, (c) M2, and (d) M3

For a better visualization of the results, Figure 11 shows the behavior of variables I_p and E_p as a function of the σ-phase concentration. Thus, it can be observed that the increase in the I_p values is associated to the increase in the content of the σ-phase in the HAZ of DSS. Such result was expected, since it can be justified by a higher concentration of the element chromium (Cr) present in the σ-phase, which also participates in the selective electrochemical reaction during LSV and contributes to the increase of I_p. On the other hand, the E_p value of the samples decreases with the increase of the content of the intermetallic phase. Such behavior was also expected, considering that element Cr present in σ-phase is more reactive and favors the early occurrence of the oxidation reactions that occur on the surface of the base metal during LSV.

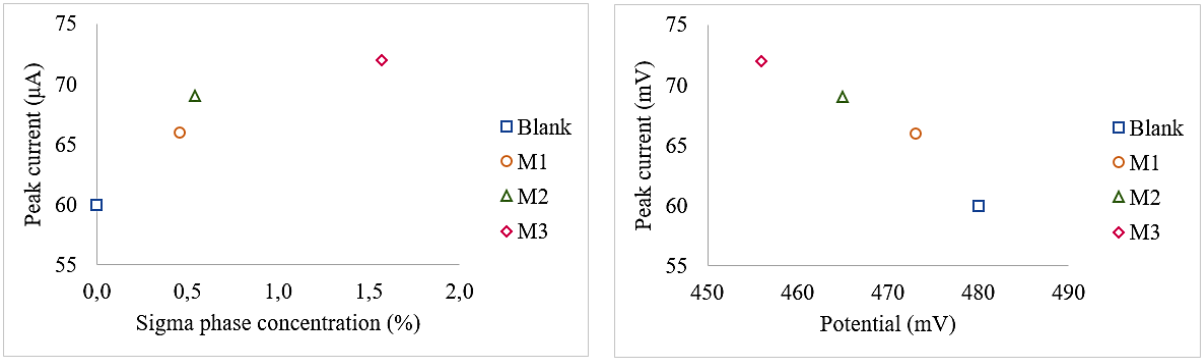

(a) (b)

Figure 11 – Variation of the peak current (a) and of the peak potential (b) as a function of the content of the σ-phase in the DSS

In view of the exposed results, it was observed that the LSV technique was effective in detecting the σ-phase in small concentrations in welded samples of DSS UNS31803. Thus, the technique proves to be promising for field applications, since it is a non-destructive test with high sensitivity for detecting the intermetallic phase.

4. CONCLUSION

The present work studied the effect of the MIG/MAG-type multipass weld in the formation of the σ-phase in UNS S31803 DSS samples. It was observed that the precipitation of the intermetallic phase had greater development in the region of the last weld pass applied to the samples under analysis, which favors the quantification of the deleterious phase using surface techniques, as the LSV technique. The experimental configuration of the electrochemical test occurred at the sweep speed of 0.5 mV s^{-1}, using a potassium hydroxide solution at a concentration of 4 mol L^{-1} as electrolyte. The technique presented good sensitivity, as it was able to detect contents related of the order of 0.45% of the σ-phase in the DSS. Another advantage of using this technique is related to the fact that it is a non-destructive test. Thus, LSV is presented as a promising technique for quantification of intermetallic phase in DSS.

5. ACKNOWLEDGEMENTS

The present study was partly funded by the Coordination for the Improvement of Higher Education Personnel – Brazil (CAPES) – Finance Code 001.

6. REFERENCES

Almeida, D.A.M., Lima, E.F.S., Ribeiro, R.L., Vieira, P.C., Alencar, R.A. and Silva, M.J.G., 2019. "Análise da formação e da microdureza predominantemente na fase intermetálica sigma em um aço inoxidável duplex SAF 2205". In *74nd annual congress of Associação Brasileira de Metalurgia, Materiais e Mineração* – ABM WEEK 2019, São Paulo, Brazil.

ASTM, 2021. *ASTM A276 – 02a. Standard Specification for Stainless Steel Bars and Shapes*. https://compass.astm.org/Standards/HISTORICAL/A276-02A.htm. Acessed 24 may 2021.

Bard, A.J., and Faulkner, L.R., 2001. *Electrochemical Methods: Fundamentals and Applications*, John Wiley & Sons, EUA.

Biezma, M.V., Martin, U., Linhardt, P., Ress, J., Rodríguez, C., and Bastida, D. M., 2021. "Non-destructive techniques for the detection of sigma phase in duplex stainless steel: A comprehensive review". *Engineering Failure Analysis*, Vol. 122, pp. 105227.

Dominices, D., Gomes, B., and Vilarinho, L. O., 2020. L. O. "Influence of present phases in corrosion and mechanical behavior of UNS S31803 duplex stainless steel welded by conventional short circuit MIG/MAG / MAG process". *Journal of Materials Research and Technology*, Vol. 9, No. 5, pp. 11244–11254.

Forteski, E.G.,2020. *Evaluation of electrochemical behavior of the sigma phase in duplex stainless steel, in Potassium hydroxide – Linear sweep voltammetry technique (in Portuguese)*. Master's Thesis, Graduate Program in Mechanical Engineering, Federal University of Paraná, Curitiba, Brazil.

García-Rentería, M.A., López-Morelos, V.H., García-Hernández, R., Dzib-Pérez, L., García-Ochoa, E.M., and González-Sánchez, J., 2014. "Improvement of localised corrosion resistance of AISI 2205 Duplex Stainless Steel joints made by gas metal arc welding under electromagnetic interaction of low intensity". *Applied Surface Science*, Vol. 321, pp. 252–260.

Granjon., 1991. *Fundamentals of welding metallurgy*. Abington Publishing, Cambridge.

Gunn, R.N., 1997. *Duplex stainless steels: microstructure, properties and applications*. Abington Publishing, Cambridge.

Haskel, H.L., Sanches, L.S., and Ponte, H.A., 2019. "A new methodology of nondestructive testing for quantitative evaluation of sigma phase in duplex stainless steels". *Materials Research*, Vol. 22, No. 3

Jebaraj, A.V., Ajaykumar, L., Deepak, C.R., and Aditya, K.V.V., 2017. "Weldability, machinability and surfacing of commercial duplex stainless steel AISI2205 for marine applications – A recent review" *Journal of Advanced Research*, Vol. 8, No. 3, pp. 183–199.

Karlsson, L., 2012. "Welding duplex stainless steels – A review of current recommendations". *Welding in the World*. Vol. 56, No. 05 pp.65–76.

Moteshakker, A. and Danaee, I., 2016. Microstructure and Corrosion Resistance of Dissimilar Weld-Joints between Duplex Stainless Steel 2205 and Austenitic Stainless steel 316L. *Journal of Materials Science & Technology*, Vol. 32, No. 3, pp. 282–290.

Olsson, C.A. and Landolt, D., 2003. "Passive films on stainless steels - chemistry, structure and growth". *Electrochimica Acta*, Vol. 48, pp. 1093–1104.

Unnikrishnan, K. and Mallik, A.K., 1987. "Aging Behavior of a Duplex Stainless Steel". *Materials Science and Engineering*. Vol. 95, pp. 259-265.

7. RESPONSIBILITY NOTICE

The authors are the only responsible for the printed material included in this paper.